FUDMA Journal of Sciences (FJS)
ISSN online: 2616-1370
ISSN print: 2645 - 2944
Vol. 8 No. 4, August, 2024, pp 79 - 89
DOI: https://doi.org/10.33003/fjs-2024-0804-2515

ROCK PHYSICS SIMULATION OF RESERVOIR SAND_K2 IN 'KUTI' FIELD, DEEP OFFSHORE NIGER DELTA

***[1]Oladele Sunday, [1]Onayemi John Ramon and [2]Rotimi Salami**

[1]Department of Geosciences, University of Lagos, Lagos, Nigeria,
[2]Olusegun Agagu University of Science and Technology, Okitipupa, Ondo State, Nigeria

*Corresponding authors' email: soladele@unilag.edu.ng

ABSTRACT

Rock physics modelling has been employed in studying the elastic behaviors of reservoir SAND_K2 in the 'KUTI' Field, Niger Delta under a plausible production scenario of increasing water saturation. The study aimed to investigate how variation in reservoir fluid saturation will influence seismic attributes and determine the characteristics of expected time-lapsed (4-D) seismic signals that may be generated due to the effects of production. Multivariate cross-plot analyses of petro-elastic parameters were carried out to establish the seismic characteristics of the target reservoir with different pore fluids in its natural state before production. Fluid replacement modelling was applied to calculate measurable changes in the reservoir's seismic characters by steadily increasing the water saturation from its initial value to 100%. Synthetic logs of petro-elastic parameters were created for different values of water saturation and combined into property cross-plots to predict the dynamic seismic response of the reservoir as brine gradually replaced hydrocarbon. Results showed that fluid changes from hydrocarbon to brine produced significant and quantifiable seismic signatures for time-lapse monitoring investigation. At some future points in the production history of the field under increasing water saturation conditions, the density, P-wave velocity and acoustic impedance of SAND_K2 increase and produce a negative seismic difference data of P-wave amplitude. Based on the responses of reservoir SAND_K2 under modelled production conditions, the study concluded that rock physics analysis can help to optimize and enhance the success of time-lapse monitoring of the KUTI Field.

Keywords: Seismic difference, Multivariate cross-plot, Petro-elastic, Time-lapsed seismic, Rock physics

INTRODUCTION

As humanity grapples with its enormous energy demands, hydrocarbon exploration is rapidly shifting to deeper waters in anticipation of finding new prospects. With maturing basins and increasingly deeper and complex frontiers, it is nowadays essential to lengthen the life of producing fields and maximize hydrocarbon recovery. In general, fluids in the reservoir interact dynamically with one another under certain geologic and anthropogenic conditions. These interactions activate variations in rock and fluid properties within a reservoir, consequently affecting its seismic response. The influence of these changes on the seismic signatures can be modelled under different geologically plausible situations to monitor the elastic behaviour of the reservoir in the couse of its production life (Onayemi *et al*., 2019). Lately, technological advancement has caused radical changes in hydrocarbon exploration and the development of oil and gas fields, making time-lapse seismic technology invaluable worldwide. The fundamental theory of time-lapse or four-dimensional (4-D) seismic is straightforward. It is a theoretically simple procedure to calculate the seismic differences between two 3-D seismic volumes. Seismic differences interpretation about likely reservoir changes related to production is based on the assumption that the surveys are repeatable. The challenges related to seismic differences produced by the usage of more than one seismic difference have been discussed extensively by Ross *et al.* (1996) and Ross *et al.* (1997).

Practically, 4-D seismic includes data gathering and analysis of repeated three-dimensional (3-D) seismic on a producing field to determine the changes that occurred in the reservoir in the couse of production. Interpretation of these changes can help maximize hydrocarbon recovery during the production life of a field. Although, acquiring this information has grim budgetary costs; increasing the recovery factor of a reservoir, even by a slight margin, has significant consequences on the business income (CGG Veritas, 2009). Irrespective of its successful application in the past decades, the conventional 4-D seismic method is susceptible to varying degrees of ambiguity that can lead to erroneous results and provide misleading information. Consequently, the inexperienced application of this technology often results in unacceptable results (Eastwood *et al*., 1998). Over-reliance on the characteristic differences between different 3-D seismic data could be responsible for the non-uniqueness of the conventional application of the 4-D seismic method. The observed seismic differences could have arisen from several other causative factors aside from reservoir-related changes (Onayemi *et al*., 2019). Such non-unique situations have been prominently linked to complex petroleum systems. As a result, the traditional time-lapse seismic exploration, on its own, is neither efficient nor reliable for monitoring complex turbidite systems and highly heterogeneous reservoirs of the deepwater Niger Delta.

The problems facing the 4-D seismic method can be successfully managed through rock physics modeling which provides prior knowledge of the characteristics of the expected production-induced reservoir's seismic signatures. It is therefore undoubtedly vital to carry out rock physics simulated experiments to map production-induced reservoir changes for development decisions. The theory and principle of physics have been discussed extensively by Avseth *et al*., (2001) and Avseth *et al*., (2005). Rock physics experiments for time-lapse seismic feasibility studies have been carried out by several workers (Avseth and Norun, 2011)

Rock physics assesses the feasibility of detecting the impact of diverse production situations on the reservoir and the possible interpretation of the associated 4-D seismic data. After establishing that the reservoir will produce a measurable 4-D seismic response, then a survey design can begin (CGG

Veritas, 2009). The non-uniqueness attribute of the conventional 4-D seismic method has motivated the application of rock physics modelling for a quantitative 4-D feasibility study of reservoir SAND_K2 in the 'KUTI' field, deep offshore Niger Delta (Figure 1). The prime objective was to estimate the types of production-induced changes that may take place in the reservoir. The intention was to generate calibrated synthetic 4-D data that can serve as important constraints for optimizing 4-D survey design in the field and to guide the interpretation of time-lapse results. 'KUTI' Field is located within the offshore section of the Niger Delta basin reported to be very prolific with large distributions of structural and stratigraphic traps. However, due to the complex nature of the deepwater setting, the reservoirs are highly heterogeneous; a condition that might contribute significantly to uncertainties in conventional 3-D exploration in the area. This study is very essential in that it helps to discriminate between 4-D anomalies generated by production effects and anomalies induced by the reservoir's heterogeneity to optimize recovery.

Geology

The geology of the Niger Delta Basin is characterized by three broad lithologies: Akata Formation, Agbada Formation and Benin Formation (Evamy *et al*.,(1978), Turttle *et al.,* (1999)). The Akata Formation is composed of predominantly over-pressured and under-compacted marine shale, which forms the base of the known delta sequence and extends across all depobelts. According to Ejedawe (1981); Turttle *et al.,* (1999); and Doust and Omatsola, (1990), petroleum occurs throughout the Agbada Formation of the Niger Delta, however, the gas-oil ratio increases southward. Most fields in the Niger Delta consist of many individual reservoirs that contain oil of varying composition with different gas-oil ratios (Turttle *et al.,* 1999). Several of the reservoirs are overpressured and gas expansion constitutes the common method of primary production (Kulke.1995). Prominent oil production problems in this region include water coning, unconsolidated sands, wax deposition and high gas-oil ratios, resulting in an ultimate recovery rate of up to 30% (Kulke. 1995).

The Niger Delta is very prolific in terms of proven oil and gas reserves. The Delta is one of the major petroleum provinces of the world, with proven recoverable reserves of approximately 26 billion bbl of oil and an under-evaluated, but probably vast gas resource base (Doust,1989, Nton and Adeyemi, 2021). The exploration of this province has taken place almost exclusively during the past decades. KUTI Field, discovered in 1996, is located in the deepwater section of the Niger Delta basin at a water depth of 1000m. Oil and gas have been produced from the Middle to Late Miocene unconsolidated turbidite sandstones of the deepwater Niger Delta since 2005. According to a report published by Gaffney, Cline and Associates (2014), 202.000 barrels per day of oil and 144 x 106 cubic ft per day of gas were produced in 2006.), 202,000 barrels per day of oil and 144 x 106 cubic ft per day of gas were produced in 2006. A recent study of the Niger Delta includes Ekom *et al.,* (2024) and Chukwuma-Orji, (2023)

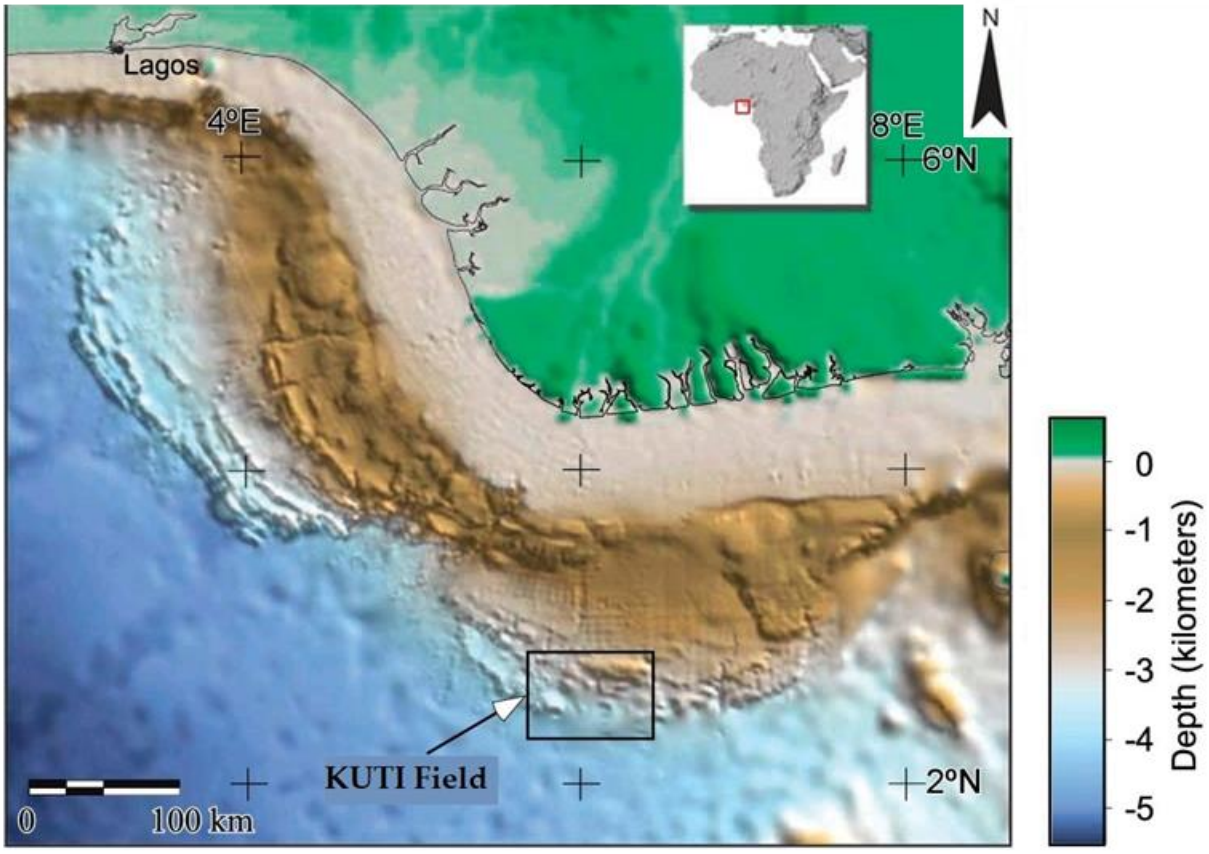

Figure 1: Sea Floor Bathymetry of the Delta showing the location of the study area (Adapted from Corredor *et al.,* 2005)

MATERIALS AND METHODS

This study has been carried out on a set of data acquired over the 'KUTI' Field, in the deep offshore Niger delta. The data consisted of four wells (KUTI-01, KUTI-02, KUTI-03 and KUTI-04) shown in Figure 2; acquired, processed and made available by Shell Nigeria. All wells, except KUTI-01, are currently suspended. Therefore, only the KUTI-01 well was analyzed and the results of reservoir SAND_K2 encountered in this well have been covered in this paper. Hampson Russell software was adopted for data visualization and interpretation. A process-based workflow, as explained below, was adopted to extract geophysical information from the available data, and to achieve the study objectives.

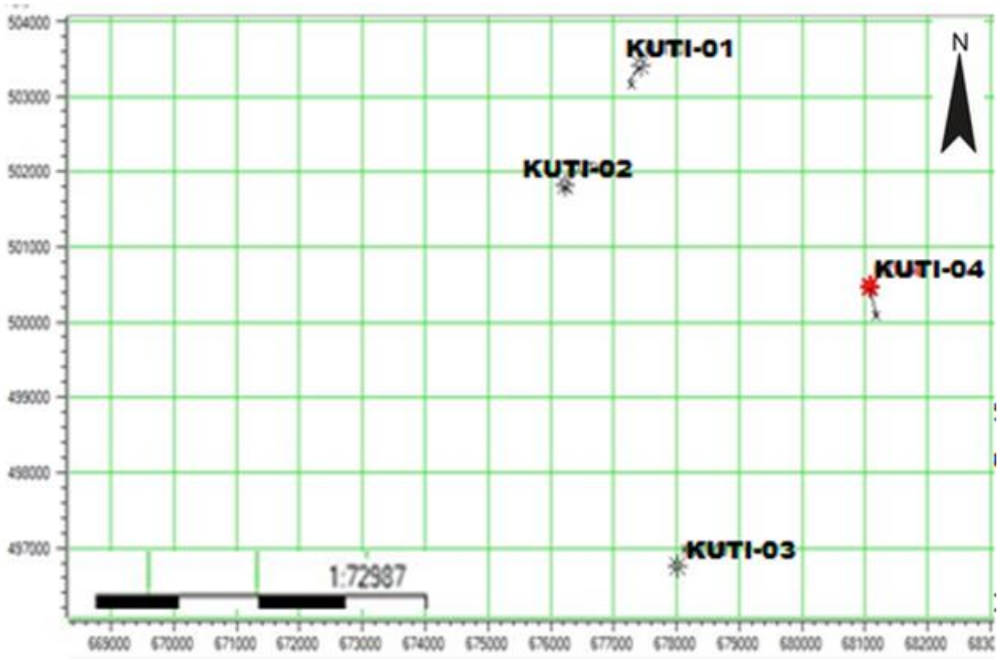

Figure 2: A map of the study area showing the spatial distribution of wells

Data Conditioning

The imported logs of KUTI-01 were examined and edited to correct for abnormalities. Subsequently, the logs were subjected to a sequence of log editing procedures, including median filtering and check shot correction. The median filtering was applied to de-spike the logs and to minimize the bogus effects caused by high-frequency noise manifesting as anomalous spikes on the log curves. The goal was to minimize the scatter obtained during cross-plot analysis.

Well Log Analysis and Petrophysics

Gamma-ray, resistivity, neutron and density logs were combined to define lithofacies, and to delineate potential reservoirs penetrated by well KUTI-01. Then SAND_K2, encountered in KUTI-01, was subjected to petrophysical evaluation to determine reservoir properties including porosity, pore fluids and fluid saturation. Other petrophysical and elastic logs such as; water saturation, porosity, S-wave velocity (Vs), P-wave velocity (Vp), Poisson Ratio, Acoustic Impedance (AI), and Lamda-Mu-Rho (LMD) were created from field logs. The shear wave was computed using the generalized Castagna model for a wet case. The resulting Shear log was further modified using Gassman's fluid replacement modelling by taking into consideration the fluid saturations of the reservoir from petrophysics.

Well-Based Rock Physics Simulation

Static Rock Physics Simulation

Multivariate cross-plot of petro-elastic properties of the reservoir were carried out to simulate the effects of different pore fluids on seismic characters of the reservoir in its natural state, before production. Three fluid-sensitive cross-plot techniques were utilized for this purpose. These include Poisson's Ratio versus Acoustic Impedance, Acoustic Impedance versus P-wave velocity, and Poisson's Ratios versus Lambda-Rho.

Poisson's Ratios versus Acoustic Impedance cross-plot – Poisson's Ratio is an advanced form of the ratios of seismic velocities (Vp/Vs), which gives a good distinction between different fluids such as gas, oil and water, owing to the high sensitivity of P-wave to fluids. Among the three main reservoir fluids, gas often displays the lowest values of Poisson's Ratios, followed by oil. Acoustic Impedance is the major component of all composite seismic data, derived from the product of P-wave velocity and density. It's also very sensitive to reservoir fluid. Owing to its higher density, brine usually has higher acoustic impedance than oil, and then gas with the least.

Acoustic Impedance versus P-wave velocity cross-plot – acoustic impedance and seismic P-wave velocity are both sensitive to reservoir fluids individually. Gas has the lowest density and, hence attenuates P-wave the most, resulting in the slowest velocity seismic waves in gas, followed by oil. Combining both into a single cross-plot gives very good discrimination between different fluids.

Poisson's Ratios versus Lambda-Rho cross-plot –Lambda-Rho is a rock physics attribute known as incompressibility, derived from P-wave and acoustic impedance. It is very sensitive to reservoir fluids because the change in pore fluids from water to hydrocarbon generally reduces the reservoir's incompressibility. The value is usually lowest in gas because gas is highly compressible, hence reducing the incompressibility of reservoirs the most, and followed by oil.

Dynamic Rock Physics Simulation

Dynamic rock physics simulation was carried out to model the effects of changing fluid saturation on seismic signatures of

the target reservoir using Gassman's fluid replacement modelling. In this study, the effect of increasing water saturation was modelled. This was achieved by varying the value of water saturation gradually from the initial reservoir brine saturation of 2.7% to 100% and then computing the logs and seismic responses of the reservoir for each value of water saturation. The resulting synthetic data were compared with the field data to predict the characteristics of 4-D anomaly induced by increasing water saturation. Also, synthetic seismic difference data was computed for each value of water saturation by subtracting the derived monitor data from the field baseline data.

RESULTS AND DISCUSSION

Reservoir Identification and Evaluation

Results of well-log analysis and petrophysical evaluation are presented in Figure 3 and Table 1.

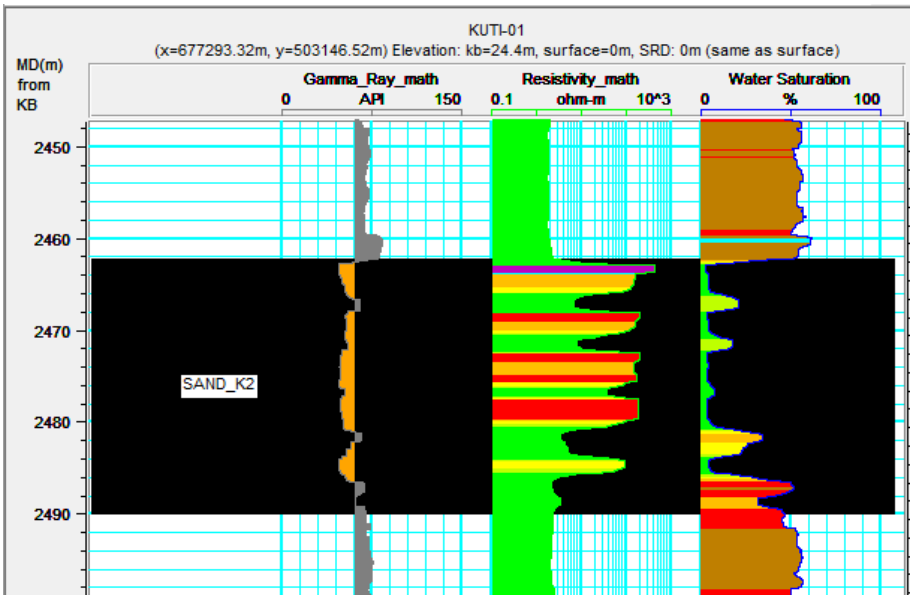

Figure 3: Location of SAND_K2 in well KUTI-01, and its petrophysical properties

Table 1: Petrophysical Evaluation of SAND_K2

Top MD (m)	Bottom MD (m)	Thickness (m)	NTG	Porosity (%)	Fluid	Sw (%)
2460.89	2494.49	32.8	0.79	33	Hydrocarbon and Brine	2.7

Seismic Attributes of SAND_K2

Multivariate cross-plot analysis of petro-elastic parameters reveals the pre-production seismic characteristics of SAND_K2 in relation to different pore fluids (Figures 4, 5 and 6). The cross-plot of acoustic impedance (AI) versus Poisson's Ratio (Fig. 5) produces three distinct cluster zones which have been interpreted, based on the water saturation color code, as gas, oil and hydrocarbon/brine zones. Gas zone is characterized by very low Poisson's ratio and AI (0.3 – 0.31 and 4250 – 4750 m/s*g/cm3 respectively) owing to low density of gas and attenuation effect of gas on compressional wave. The oil zone has slightly higher values of Poisson's ratio and AI; 0.32 – 0.33 and 5000 – 5250 m/s*g/cm3 respectively. The hydrocarbon/brine zone has the highest values of Poisson's and AI; 0.32 – 0.33 and 5500 – 5750 m/s*g/cm3 respectively. The presence of higher density brine in the hydrocarbon/brine zone is responsible for the high values of Poisson's ratio and AI in this zone.

Similarly, cross-plot of Lambda-Rho versus Poisson's Ratio (Fig. 5) produces three distinct cluster zones which have been interpreted as gas, oil and hydrocarbon/brine zones. The gas zone has the lowest Lambda-Rho values of 15 – 16 Gpa*g/cm^3. This is so because gas is the most compressible of all reservoir fluids, and its presence in the reservoir's pore spaces has a significant effect on reducing the incompressibility of the reservoir, which is reflected by the very low values of Lambda-Rho. The oil zone has Lambda-Rho values of 17 – 18 Gpa*g/cm^3.

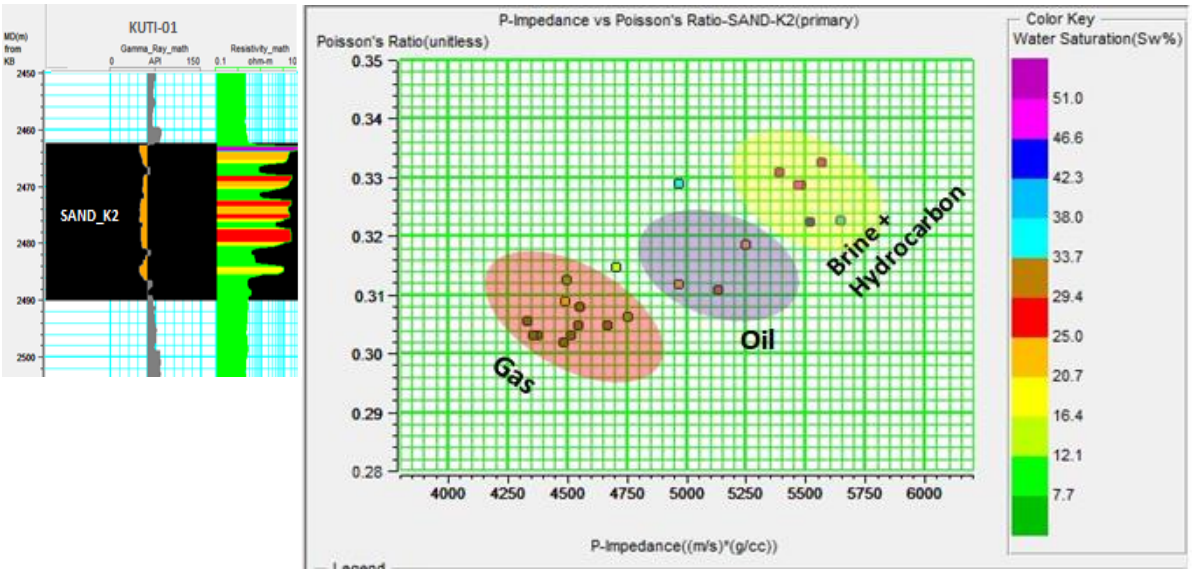

Figure 4: Multivariate cross-plot of Acoustic Impedance (P-impedance) versus Poisson's Ratio colour-coded with Water Saturation for SAND_K2

The hydrocarbon/brine zone has the highest Lambda-Rho value of greater than 20 Gpa*g/cm^3. Water is the least compressible fluid, and thus affects the reservoir's incompressibility the least. Therefore, the presence of brine in the hydrocarbon/brine zone is the primary cause of the highest value of Lambda-Rho. The cross-plot of Acoustic Impedance (AI) versus P-wave Velocity (Vp) in Figure 6 produces three distinct cluster zones which have been interpreted as gas, oil and hydrocarbon/brine zones. The gas zone has the lowest Vp values of 2100 – 2200 m/s due to the attenuation effect of gas on compressional waves. Also, P-wave travels slower in gas compared to oil and brine. Oil has Vp values of 2200 – 2300 m/s. The hydrocarbon/brine zone has the highest Vp values (>2400 m/s). Among the reservoir fluids, water transmits P-wave the most. Therefore, its presence in the hydrocarbon/brine zone is responsible for the highest value of Vp in this zone. The pre-production seismic attributes of SAND_K2 concerning different pore fluids are tabulated in Table 2.

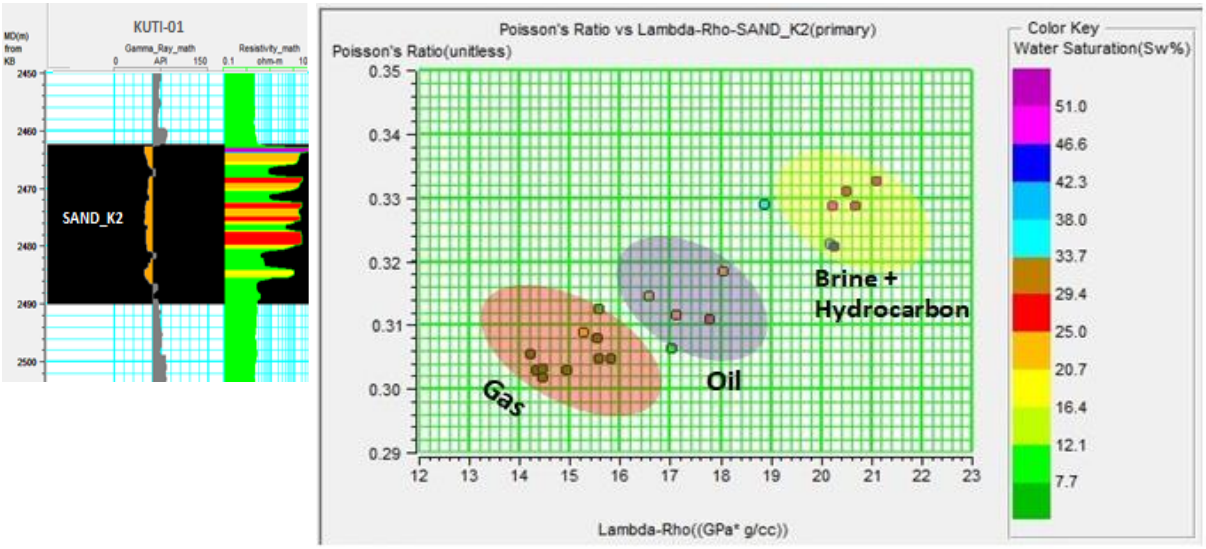

Figure 5: Multivariate cross-plot of Lambda-Rho versus Poisson's Ratio colour-coded with Water Saturation for SAND_K2

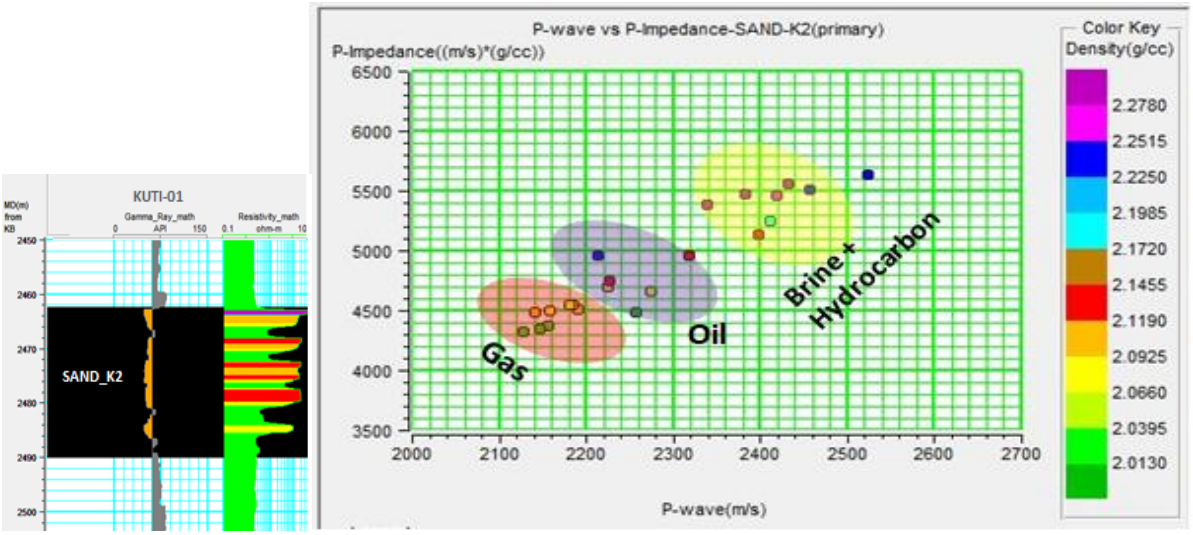

Figure 6: Multivariate cross-plot of Acoustic Impedance (P-impedance) versus P-wave velocity colour-coded with Water Saturation for SAND_K2

Table 2: Pre-production Seismic Attributes of SAND_K2 with different pore fluids

AI(ms)*(g/cm^3**)** **Gas/ Oil/ Brine**	**Poisson's Ratio Gas/ Oil/ Brine**	**P-wave (m/s) Gas/ Oil/ Brine**	**Lambda-Rho (GP*** g/cm^3**) Gas/ Oil/ Brine**
4250 – 4270	0.30 – 0.31	2100 – 2200	15 – 16
5000 - 5250	0.31– 0.31	2200 - 2300	17 – 18
Above 5500	Above 0.32	Above 2400	Above 20

4D Analysis of SAND_K2

Figure 7 shows the dynamic effects of increasing water saturation on elastic logs along the interval of SAND_K2. All logs showed a progressive increase in seismic attributes as the water saturation gradually tends towards 100% from the initial reservoir value of 2.7%. Multivariate cross-plots (Figs. 8 - 11) of these synthetic attributes (Acoustic Impedance (AI), P-wave velocity (Vp) and Density) linked the observed changes in seismic attributes (4-D effects) to corresponding variation in water saturation. As the value of water saturation gradually increases from 2.7 % to 100%, the data points move in the direction of increasing AI, Vp and density. Also, the impedance contrast within the reservoir decreases continuously as brines continue to replace hydrocarbon. At 100% water saturation, the impedance contrast becomes nearly immeasurable as the reservoir becomes fully saturated with brine. The characteristic 4-D seismic signals of the reservoir about the production effect of increasing water saturation are summarized in Table 3. An anomalous change in P-wave velocity can be observed between 22.7% and 62.7% water saturation. The P-wave velocity increases as water saturation is gradually increased from 2.7% to 22.7%. However, the Vp decreases unexpectedly as the water saturation increases to 42.7%. Beyond this, the Vp starts to increase again and continuously as the water saturation approaches 100% (Table 3).

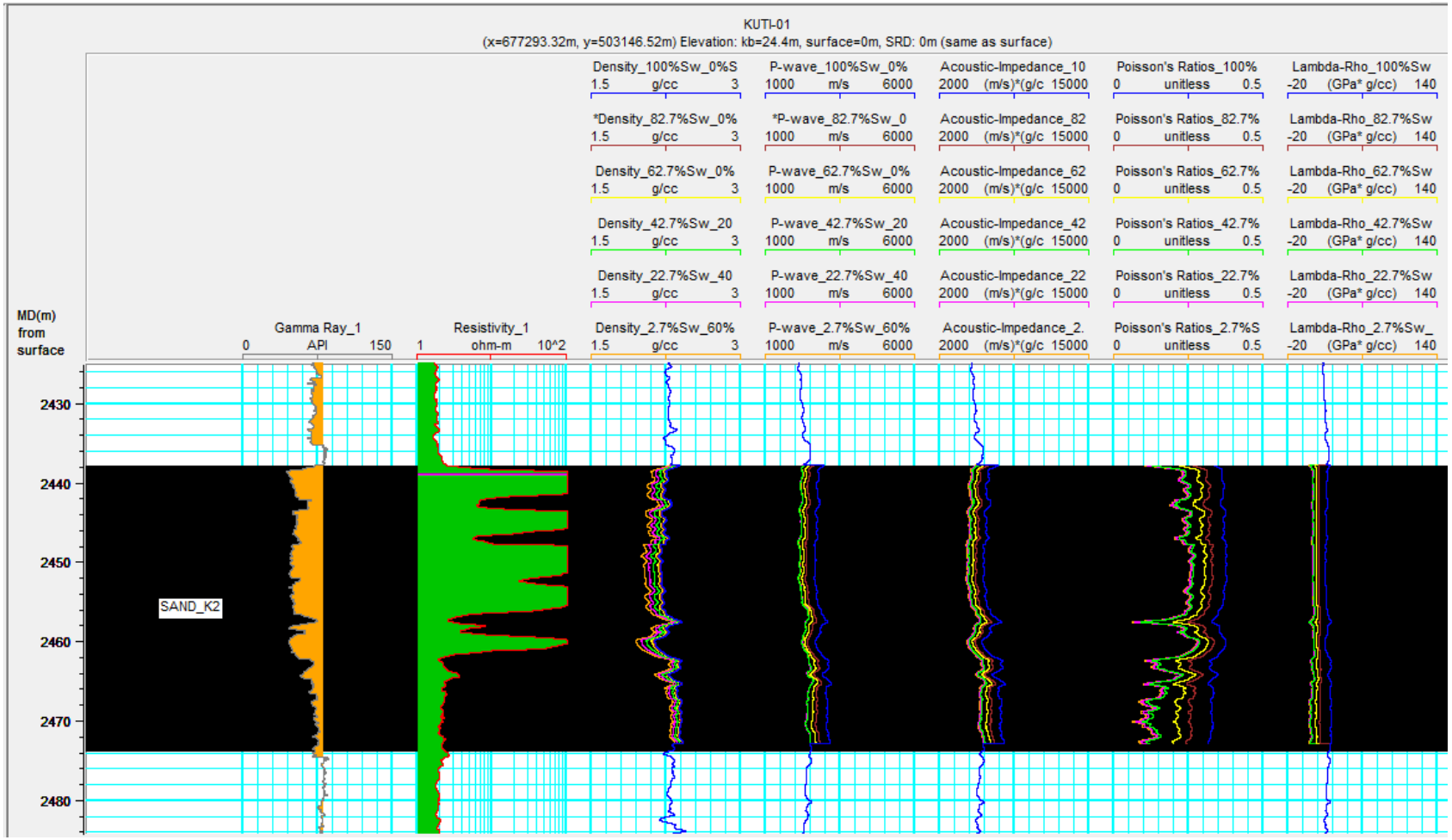

Figure 7: Results of Fluid Replacement Modeling of SAND_K2 with 20% increase of water saturation from initial reservoir value of 2.7% to 100%: 2.7% (orange curve,) 22.7% (magenta curve), 42.7% (green curve), 62.7% (yellow curve), 82.2% (red curve) and 100% (blue curve) brine saturations. The original logs are at 2.7% water saturation, 38.3% oil saturation and 60% gas saturation

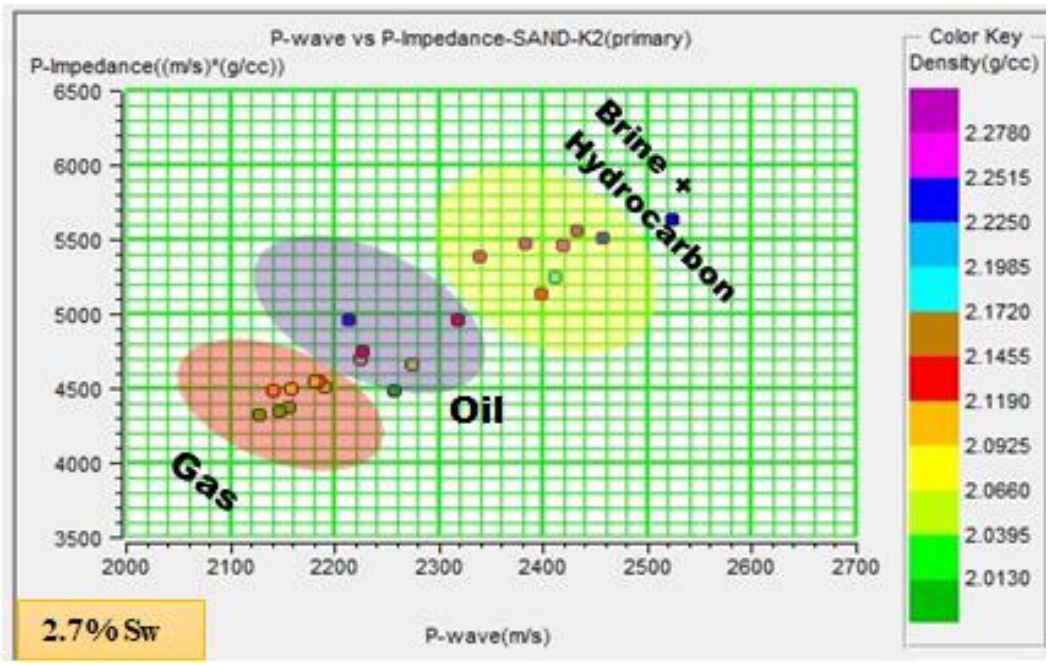

Figure 8: Multivariate cross plot of Acoustic Impedance vs. P-wave Velocity (Colour coded with density) showing the seismic response of reservoir SAND_K2 to the initial water saturation value of 2.7%

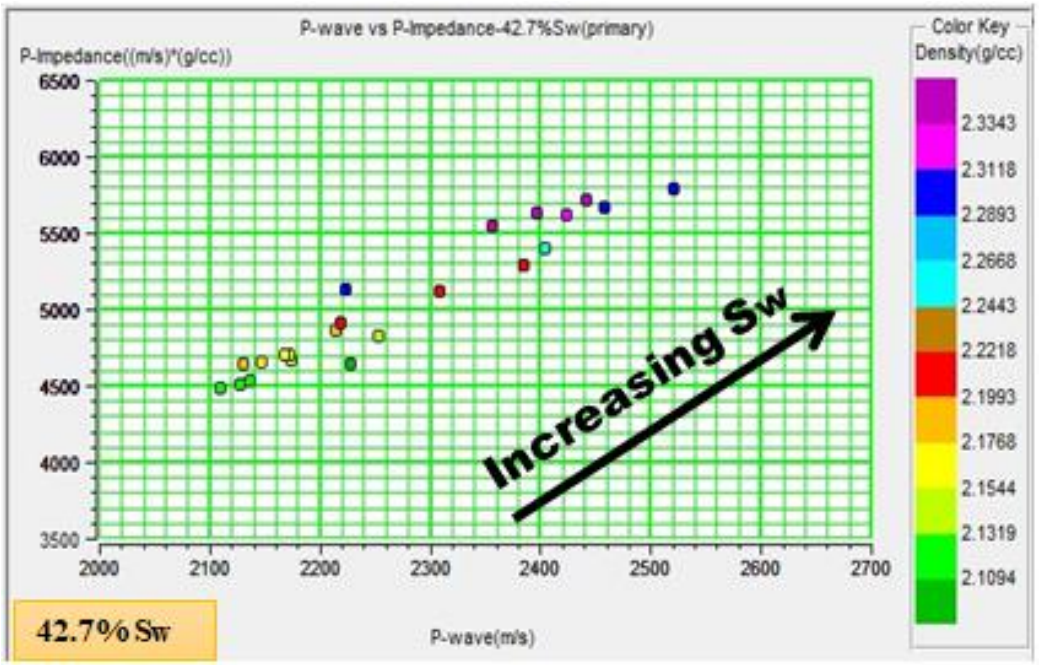

Figure 9: Multivariate cross plot of Acoustic Impedance vs. P-wave Velocity (Colour-coded with density) showing the seismic response of reservoir SAND_K2 to the water saturation value of 42.7%

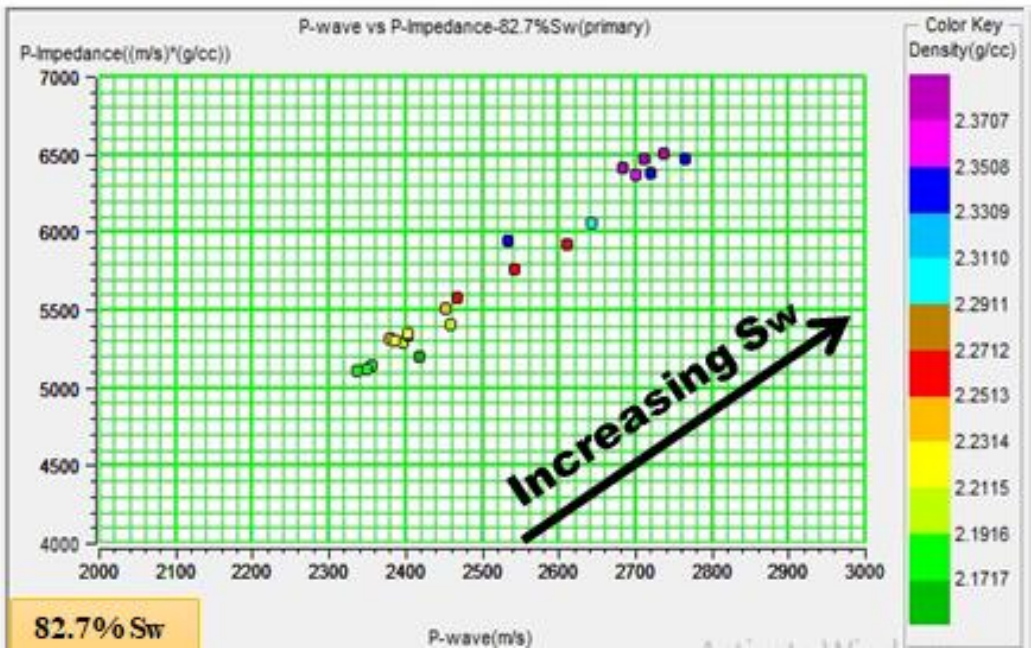

Figure 10: Multivariate cross plot of Acoustic Impedance vs. P-wave Velocity (Colour coded with density) showing the seismic response of reservoir SAND_K2 to the water saturation value of 82.7%

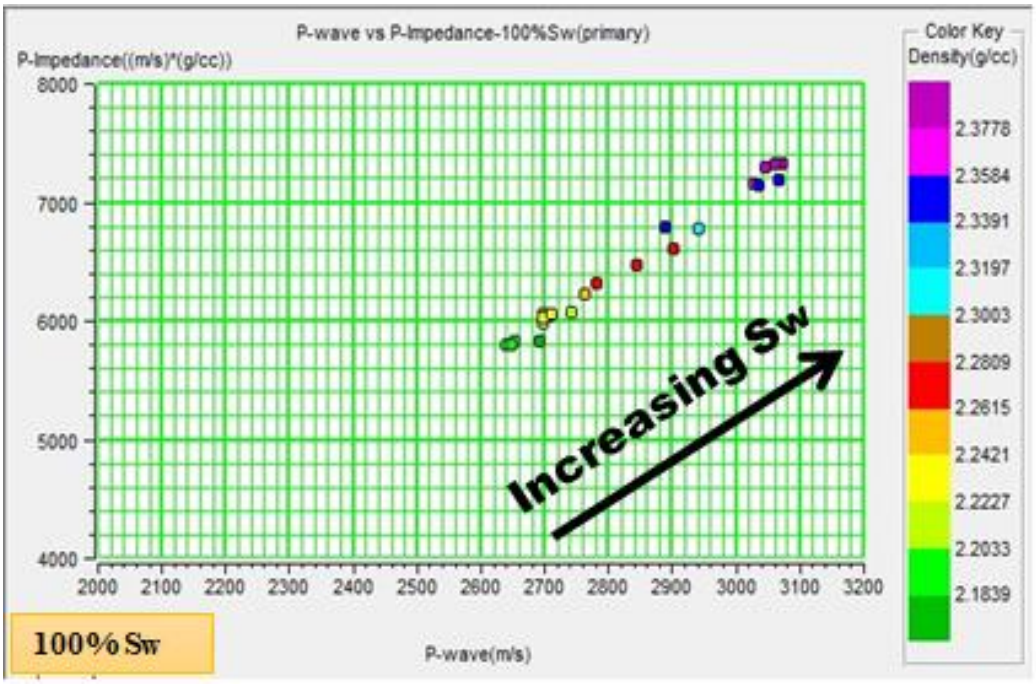

Figure 11: Multivariate cross plot of Acoustic Impedance vs. P-wave Velocity (Colour coded with density) showing the seismic response of reservoir SAND_K2 to the water saturation value of 100%

Table 3: Characteristic 4-D seismic signals produced by SAND_K2 for each value of water saturation

	FIELD (BASE) DATA 2.7% Water	**SYNTHETIC (MONITOR) DATA**				
		22.7% Water	**42.7% Water**	**62.7% Water**	**82.7% Water**	**100% Water**
Average Vp	2208	2358	2224	2408	2549	2910
Average AI (m/s)*(g/cc)	5037	5445	5197	5695	6048	6926
ΔVp (BASE - MONITOR)	0	-149	-15	-200	-340	-701
ΔAI (BASE - MONITOR)	0	-407	-160	-658	-1010	1888

CONCLUSION

A well-based rock physics modelling has been applied successfully to determine the seismic signatures of SAND_K2, before production and to study the dynamic behaviour of the reservoir under a plausible production scenario of increasing water saturation. In general, SAND_K2 is characterized by three fluids, oil, gas and brine. The seismic characters of the gas-filled pores, in terms of average acoustic impedance and P-wave velocity, are 4260 m/s*g/cm^3 and 2150 m/s respectively, while that of the oil-filled pores are 5125 m/s*g/cm^3 and 2250 m/s respectively. The presence of brine in the hydrocarbon/brine-filled pores increases the acoustic impedance and P-wave velocity above 5500 m/sec*g/cm^3 and 2400 m/s respectively. Increasing the water saturation of the reservoir gradually from its original value of 2.7% resulted in a corresponding increase in P-wave velocity, density, acoustic impedance, Poisson ratio and Lambda-Rho. At water saturation of 25%, 50%, 75% and 100%, the acoustic impedance of the hydrocarbon-filled zone increased by 100 (m/s)*(g/cm^3), 250 (m/s)*(g/cm^3), 300 (m/s)*(g/cm^3) and 450(m/s)*(g/cm^3) respectively. The anomalous change in P-wave velocity between 22.7% and 62.7% water saturation can be attributed to the sudden change in pore pressure as gas comes out of solution owing to the replacement of gas by brine. This anomaly can be investigated further using pressure data. The result of fluid replacement modelling revealed that increasing water saturation of SAND_K2 in well KUTI-01 (a similar condition to production scenarios) would produce significant and detectable 4-D signals for a time-lapse monitoring survey. At some future points in the production history of the field under increasing water saturation conditions, the acoustic impedance of SAND_K2 will increase due to an increase in its P-wave velocity and density. Also, increasing water saturation will produce negative seismic difference data of P-wave amplitude for time-lapse analysis.

REFERENCES

Adeniji, A. A., Titus, E. A., Onayemi, J. R. (2020): Application of rock physics technology for 4- D monitoring of a siliciclastic reservoir in Offshore Niger Delta Basin. American Geophysical Union, Fall Meeting 2019. https:!/ui.adsabs.harvard.edu/abs/20 AGUFMMR21 C0080A/abstract.

Avbovbo, A. A., (1978): Tertiary lithostratigraphy of Niger delta: American Association of Petroleum Geologists Bulletin.v. 62, p. 295-306.

Avseth, P. and NorunrrSkjei, (2011): Rock physics modelling of static and dynamic reservoir properties - A heuristic approach for cemented sandstone reservoirs. The Leading Edge' January 2011. DOI: *10.1190/1.3535437.*

Avseth. P., Mukerji, T. and Mavko, G., (2005): Quantitative Seismic Interpretation: Applying Rock Physics Tools to Reduce Interpretation Risk, *Cambridge University Press.*

Avseth, P., Mukerji. T., Mavko. G., and Tyssekvam, J. A., 2001: Rock Physics and AVO analysis for Lithofacies and Pore Fluid Prediction in a North Sea oil field. *The Leading Edge,* 20.429.

Ayiaz, K., Adam Koesoemadinata, Nick Moldoveanu, N Nikita C. and Yusuf B. A., (2018): Application of an Efficient Workflow for 4D Time-lapse Seismic Feasibility Analysis. *SEG International Exposition and 88th Annual Meeting.10.1190/segam2018- 2997263.1. Pg 5318 – 5322.*

Chukwuma-Orji J. N. (2023): The Sedimentological Analysis, Depositional Environment and Sequence Stratigraphic Study of Ida 4, 5, 6 Wells Niger Delta Basin, Nigeria. *FUDMA Journal of Sciences*, *7*(5), 296 - 317. https://doi.org/10.33003/fjs-2023-0705-1975

Corredor, F., Shaw, J.H and Bilotti F., (2005): Structural Styles in the dee -water fold and thrust belts of the Niger Delta. *AAPG Bulletin,* 89, (6), 753-780.

Doust, H and Omatsola, E., (1990): Niger Delta," In J. D. Edwards and P. A. Santogrossi. Eds., Divergent/Passive Margin Basins: *American Association of Petroleum Geologists Memoir, Vol. 48, 1990, pp. 201-238.*

Doust, H., (1989): The Niger Delta: hydrocarbon potential of a major Tertiary delta province, Coastal Lowlands. Springer, Dordrecht. https://doi.org/10.1007/978-94-017-1064-0_13

Eastwood, J., Johnston, D., Huang, *X.*, Craft. K., Workman. R., (1998): Processing for Robust time-lapse seismic analysis: Gulf of Mexico example, Lena Field. Society of Exploration Geophysicists SEG Technical Program Expanded Abstracts 199. DOl:10.119011.1820376.

Ejedawe, J. E., (1981): Patterns of incidence of oil reserves in Niger delta basin: American Association of Petroleum. Geologists Bulletin, v. 65, p. 1574-1585.

Ekom, J. C., Alkali Y. B., Goro, A. I., & Uneuhvo, C. I. (2024): Palynological, Paleoenvironmental and Paleoclimate Analyses of Emi-5-Well, Offshore Niger Delta, Nigeria. *FUDMA Journal of Sciences*, *8*(3), 18 - 29. https://doi.org/10.33003/fjs-2024-0803-2471

Evamy, B. D., Harernboure, L Kamerling, P., Knaap, W. A., Molloy, F. A., and Rowlands. P. H.,1978. Hydrocarbon habitat of Tertiary Niger delta: American Association of Petroleum Geologists Bulletin, v. 62, p. 1-39.

Gaffney, Cline and Associates, (2014): Deepwater Nigeria; Definition of Stratigraphic Plays. *The Royal Institution Report, 29/h January. 201-1.*

Kulke, H., (1995): Regional Petroleum Geology of the World. Part II: Africa. America, Australia and Antarctica: Berlin, GebruderBorntrager. P. 143-172.

Merki, P.J., (1971): Structural geology of the Cenozoic Niger delta, *in* 1st Conference on African Geology Proceedings: Ibadan University Press, p. 635-646.

Nton, M. E., and Adeyerni, M. O., (2021): Evaluation of Hydrocarbon Reserves in AD Field. Offshore Niger Delta. Open Journal of Geology, 11. 155-174. Doi:10.4236/ojg.2021.115009.

Onayemi, J., Adeniji, A., Osinaike, A., (2019): Rock physics template modelling for time-lapse seismic analysis of reservoir M 1 in Moremi Field, Offshore Niger Delta Basin. SEG International Exposition and AIIDual Meeting, San Antonio. Texas, USA. https//:doi.org/l0.1190/segam2019-3215797.1

Ross, C.P., Cunningham, G.B., and Weber, D.P., (1996):

Inside the crosse utilisation black box. The Leading Edge, 15, 1233-1244.

Ross, C. P., S. Altan, et al., (1997): Time-lapse seismic monitoring: Repeatability processing tests: Presented at the Offshore Technology Conference, Offshore Technology Conference.

Short, K. C; and Stauble, A. J., (1967): Outline of the geology of Niger delta. American Association of Petroleum Geologists Bulletin, v. 51. p. 761-799.

Turttle, L. W. M; Brownfield, E. M: and Charpentier, R. R.., (1999): Niger Delta Petroleum System: Niger Delta Province. Nigeria, Cameroon and Equatorial Guinea, Africa. US Department of the Interior, US Geological Survey.

Weber, K. I. and Daukoru, E. (1975): Petroleum geology of the Niger Delta: Tokyo, 9th World Petroleum Congress Proceedings.v. 2, p. 209-22l.

Whiteman, A. (1982): Nigeria-its petroleum geology, resources and potential. London, Graham and Trotman, p.394.